CONF-960543--38
GA-A22352

VISIBLE SPECTROSCOPY IN THE DIII-D DIVERTOR

by
N.H. BROOKS, D. FEHLING, D.L. HILLIS,
C.C. KLEPPER, N. NAUMENKO, S. TUGARINOV,
and D.G. WHYTE

JUNE 1996

GENERAL ATOMICS

DISCLAIMER

GA–A22352

VISIBLE SPECTROSCOPY IN THE DIII–D DIVERTOR

by
N.H. BROOKS, D. FEHLING,* D.L. HILLIS,*
C.C. KLEPPER,* N. NAUMENKO,† S. TUGARINOV,‡
and D.G. WHYTE△

This is a preprint of a paper to be presented at the 11th Topical High Temperature Plasma Diagnostics Conference, May 12–16, 1996, in Monterey, California, and to be published in *Rev. Sci. Instrum.*

*Oak Ridge National Laboratory, Oak Ridge, Tennessee.
†Institute of Physics, Minsk, Belarus.
‡TRINITI Laboratory, Troitsk, Russia.
△INRS — Energie et Materiaux, Varennes, Quebec, Canada.

Work supported by
the U.S. Department of Energy
under Contract Nos. DE-AC03-89ER51114
and DE-AC05-96OR22464

GA PROJECT 3466
JUNE 1996

ABSTRACT

Spectroscopy measurements in the DIII–D divertor have been carried out with a survey spectrometer which provides simultaneous registration of the visible spectrum over the region 400–900 nm with a resolution of 0.2 nm. Broad spectral coverage is achieved through use of a fiberoptic transformer assembly to map the curved focal plane of a fast (f/3) Rowland-circle spectrograph [Tugarinov, et al., Rev. Sci. Instrum. **66**, (1995) 603] into a rastered format on the rectangular sensor area of a two-dimensional CCD camera. Vertical grouping of pixels during CCD readout integrates the signal intensity over the height of each spectral segment in the rastered image, minimizing readout time. For the full visible spectrum, readout time is 50 ms. Faster response time (<10 ms) may be obtained by selecting for readout just a small number of the twenty spectral segments in the image on the CCD. Simultaneous recording of low charge states of carbon, oxygen and injected impurities has yielded information about gas recycling and impurity behavior at the divertor strike points. Transport of lithium to the divertor region during lithium pellet injection has been studied, as well as cumulative deposition of lithium on the divertor targets from pellet injection over many successive discharges.

INTRODUCTION

This paper describes the characteristics of an innovative visible survey spectrometer formed by the marriage of a modern CCD detector to a stigmatic, Rowland-circle, survey spectrograph with high resolution and high optical throughput.[1] Initial measurements with this instrument of plasma phenomenon in the divertor of the DIII–D tokamak are reported.

With the development of multichannel photodiode arrays, the evolution of visible light, survey spectroscopy shifted from reliance on photographic film and plates to electronic detection methods. The linear photodiode arrays, or optical multichannel analyzers (OMAs) as the combination of detector and digital electronic recording were called, were available initially with a maximum length of only 25 mm. The pioneering designers of the new electronic survey instruments met the challenge of small detector size by creating flat-field spectrographs[2] in which the full spectrum was compressed to match the length of available OMAs. The concurrent maturation of holographic ruling technology was essential to the production of the aberration-corrected gratings on which the flat field spectrograph relied. Spectrometer development took a different path in the Soviet Union and East Bloc countries where multichannel photodiode detectors did not become generally available to the scientific community until a decade later than in the West. Instead of concentrating on flat field spectrographs, designers of optical instruments

in the East applied the holographic grating technology to improve the performance of conventional optical instruments with photographic recording. The properties of stigmatic imaging, high resolution and high optical throughput that resulted from that alternate path in grating development are combined with electronic detection in the spectrometer described in this paper.

I. HARDWARE DETAILS

Figure 1 is an optical schematic of the spectrometer. Light enters the spectrometer through the entrance slit at the top of the picture. The slit width is adjustable from 10 microns to 1 mm, its height is 10 mm, and the vertical resolution of its stigmatic image in the focal plane is 0.1 mm. A planar mirror deflects the light toward the grating whose aperture may be masked in the vertical direction with a choice of diaphragms. Scattered light inside the instrument is minimized with a light trap for the zero order reflection from the grating. For the 1200 G/mm grating the 140-mm-long curved input tip of the fiberoptic transformer intercepts the diffracted light between 400 and 900 nm; this 500 nm spectral swath is spread across twenty fiber conduits which are geometrically rearranged at the output tip of the transformer into a rastered rectangular array 6.7 mm wide by 13 mm high. A transfer lens assembly relays this image onto the face of the CCD sensor. A 40 mm square filter may be inserted into the collimated section of the transfer lens assembly.

Figure 2 is a photograph of the survey spectrometer with its cover removed. The main optical components described in the paragraph above may readily be identified. The circle filled with a splash of color is the concave grating, its full aperture exposed by the horizontal orientation of the slotted diaphragms above and below. Just a little farther to the right, in the horizontal midplane of the instrument, lies the fiberoptic transformer; a wavy sheet of black vinyl protects the loose glass fibers

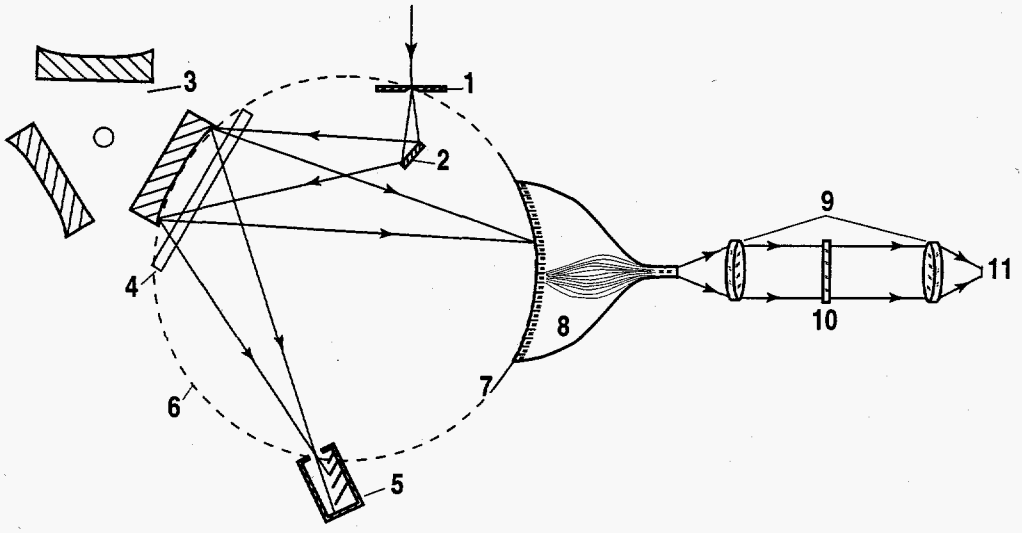

Fig. 1. Optical schematic of visible survey spectrometer where component elements by number are: 1 — entrance slit, 2 — planar mirror, 3 — grating turret, 4 — diaphragm, 5 — trap for zero order light, 6 — Rowland circle, 7 — photographic mask, 8 — fiberoptic transformer, 9 — transfer lenses, 10 — filter, 11 — CCD sensor chip.

which connect its clamped end tips. The gray cylindrical tube encloses the adjustable transfer lenses; the white box at the extreme right is the CCD camera head.

The insert in the top middle of Fig. 2 is a color photograph of the rastered spectrum at the output tip of the transformer when the spectrometer is illuminated with the continuous spectrum from a tungsten-halogen light source. This image is rotated 90° from the true orientation of the transformer output tip, such that wavelength increases with height in each vertical band. The black lines separating each of the twenty bands is the cement between conduits. The eight leftmost conduits appear white because the absence of the spectrometer's cover exposed the transformer's curved input tip to the glowing face of the video monitor. The small imperfections visible in the individual fiber conduits result from manufacturing difficulties associated with conduits having a thickness of only 0.65 mm. The precision of the coherent

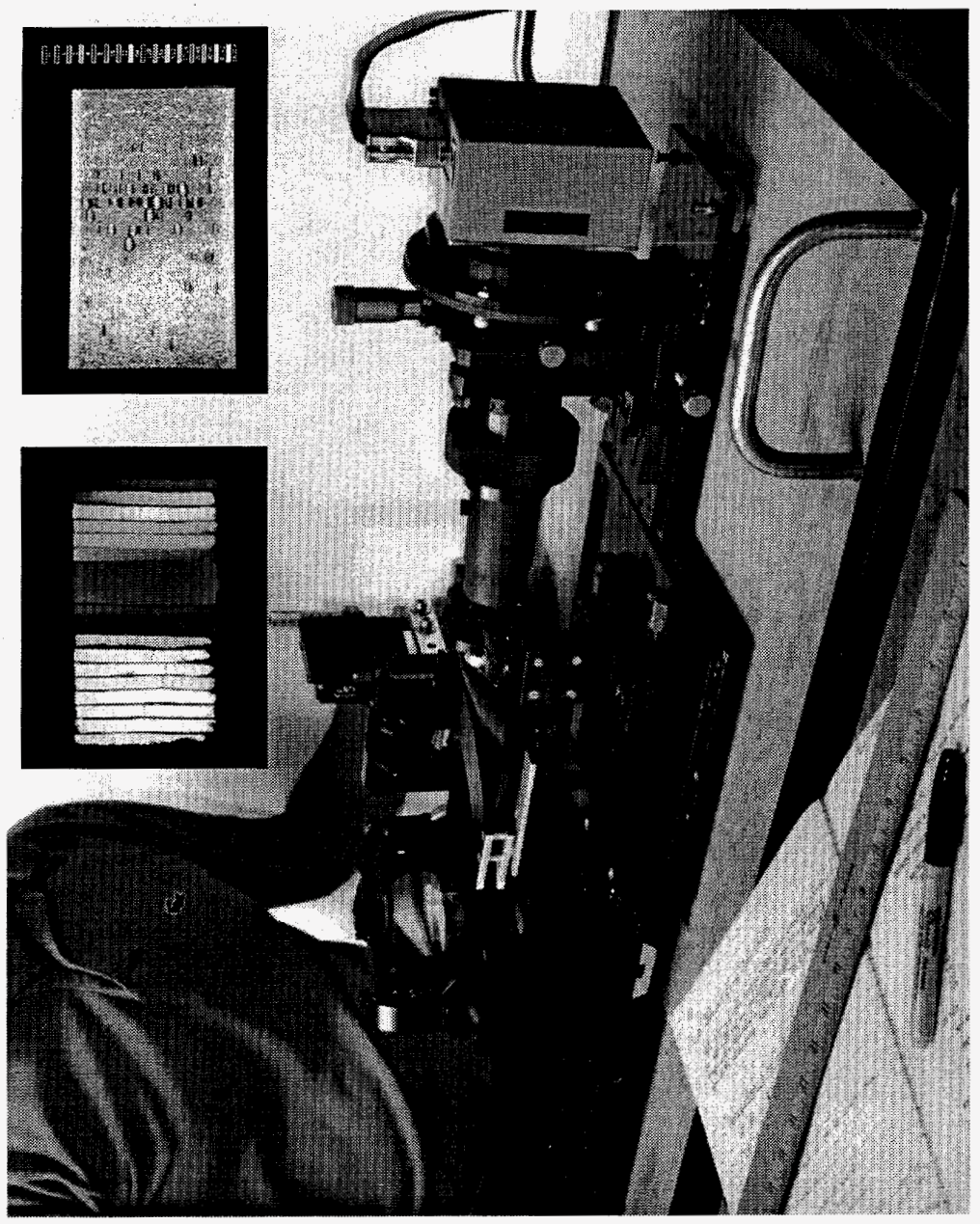

Fig. 2. Photograph of uncovered spectrometer with true color image of transformer output tip (insert top center) for spectrometer illumination with continuum light source, and false color image of PC display (insert top right) with neon light source.

transformation from input to output would be greatly improved by the use of thicker conduits than were employed in this prototypical instrument.

The insert in the top right corner of Fig. 2 is the false color display generated on the PC monitor from illumination of the spectrometer with a low-pressure neon light source. The different colors of the concentric oval contours marking each spectral line denote intensity according to the logarithmic color scale on the right. Comparing the false color image of the neon line spectrum with the true color image of the visible continuum, it is evident that the neon light source emits most strongly in the red region of the spectrum.

The 2-D detector used in this spectrometer is a Wright Instrument CCD camera with Peltier-cooled sensor operated in frame transfer mode. The image area of the sensor consists of 298 × 576 pixels, each pixel being 22.5 μm square. Vertical binning is employed to sum light from the 24 video scan lines spanned by a single spectral band or track, and vertical skipping to ignore signal from the five scan lines spanned by the cement between tracks. Bleeding of a spectral line image along the column direction of the CCD sensor occurs when the signal produced by a very bright spectral line, such as D_α, saturates the charge storage capacity of individual pixels. The insertion of a photographic mask in front of the fiberoptic transformer permits the selective attenuation of bright lines, thereby avoiding crosstalk between tracks due to saturation. Selective attenuation of the very bright D_α and D_β lines from the tokamak plasma prior to registration on the CCD camera also increases the effective dynamic range of the detector by the optical density attainable with conventional negative-image, 16 mm motion picture film,

an enhancement of at least 12 bits to the already wide, 15 bit range of the Wright camera.

A typical tokamak spectrum from a single track is shown in Fig. 3. With the spectral band of a single track dispersed over 298 pixels, the 500 nm represented by all twenty tracks in the image is spread over nearly 6,000 pixels. The expanded profile of the D_β line, lower left, is fitted with a Gaussian, the adjacent background modeled by a polynomial. The full width of the Gaussian fit at i/e is 3.0 pixels, or 0.2 nm; the spectral line width is roughly constant throughout the entire 500 nm range of the instrument. The expanded profile of a typical neutron-induced noise spike, lower right, is fitted in like fashion to D_β its full width is 1.5 pixels. Their usually narrow profile and random location in different time frames makes it possible to identify and eliminate almost all of the neutron-induced noise events during post-processing of the digitized data.

The minimum time to read out all twenty tracks is ~50 ms, if the Wright interface electronics is controlled with a 100 MHz Pentium PC. In practice, the amount of light collected from the tokamak plasma and transmitted fiberoptically to the spectrometer which sits outside the neutron shield wall precludes operation with integration times less than 100 ms. For bright features, much shorter integration times may be achieved by reading out only a couple tracks. For any pair of tracks the readout time imposed by hardware is ~5 ms.

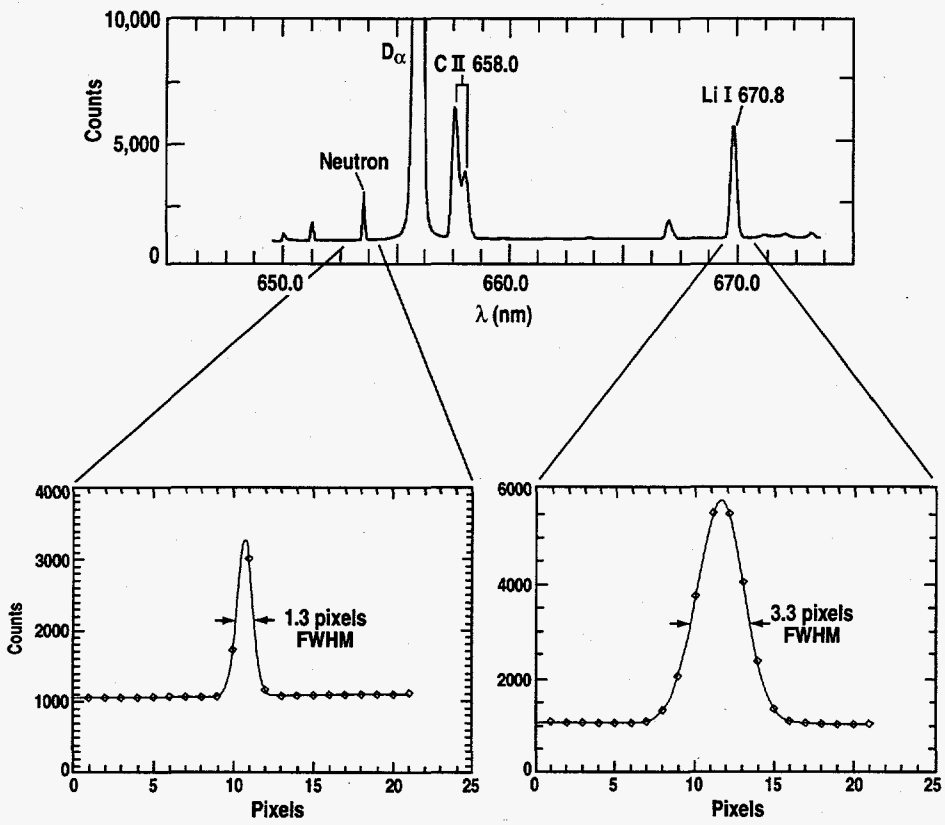

Fig. 3. Typical spectrum from tokamak obtained by summing 24 video lines spanned by a single track. Gaussian fit to Db line in lower left shows different FWHM than fit to neutron-induced noise spike in lower right.

II. RESULTS FROM LITHIUM PELLET INJECTION INTO DIII–D DISCHARGES

The first two traces in Fig. 4 shows the time behavior of lithium light at the lower outer strike point of beam-heated, double-null discharges into which lithium pellets were injected following the peaking of stored energy during the negative central shear (NCS) phase from 700 to 2200 ms — NCS plasmas are characterized by both a high q-value (safety factor) on axis and a local minimum in their radial q-profile; most importantly, they exhibit classical-like ion confinement over a large fraction of the plasma core.[3] To afford good time resolution for seeing the steplike rise and exponential decay of both Li I 670.8 and Li II 548.5 immediately following each pellet injection, the camera was configured for readout of just two tracks. During the time of lithium ablation and subsequent pumpout from the core, Li II provides a more sensitive indication than Li I of the lithium streaming from the midplane to the divertor target along diverted flux lines. On the other hand, during the reproducible quiescent L–mode phase prior to 700 ms in each shot, the intensity of Li I gives a better indication of the lithium exposed to plasma bombardment from deposition on the surface of the outer divertor target as a result of pellet injection in prior discharges. In the third box,, the Li III charge exchange line from the XUV SPRED spectrometer viewing the core plasma is displayed for comparison.

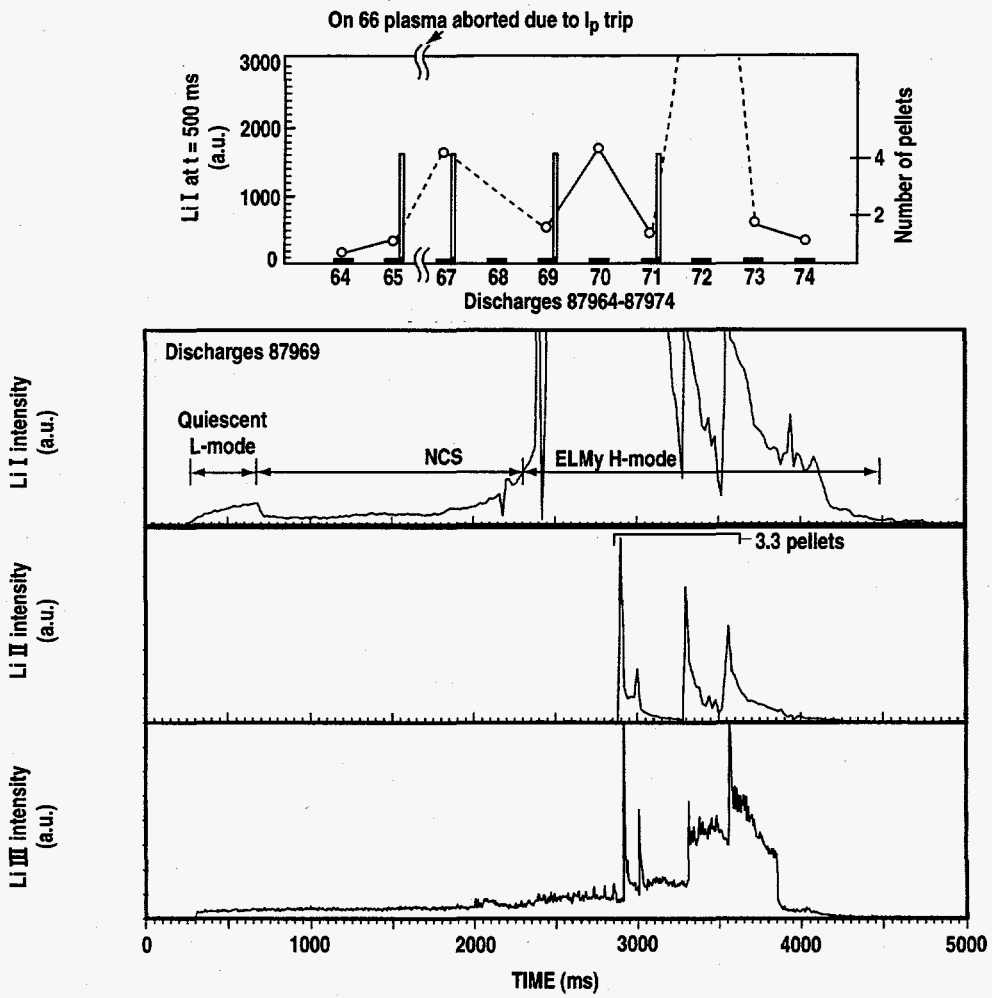

Fig. 4 Comparison of spectral line behavior of Li I and Li II from divertor target region and Li III from the core region during beam-heated, double-null discharge with lithium pellet injection during ELMy period after Negative Central Shear (NCS) phase; correlation versus shot number (insert top center) of Li I signal at t = 500 ms with number of pellets injected during late phase of preceding shot.

The insert in the top box of Fig. 4 demonstrates the clear correlation with shot number between the sputtered Li I signal at t = 500 ms in the reproducible, early quiescent L–mode phase and the number of pellets injected during the late phase of the preceding shot. This correlation is evidence that plasma bombardment of the target surface during intervening discharges either buries the lithium introduced with pellets or transports it radially outside the 20-mm-diameter view of the visible

survey spectrometer. Wall conditioning by lithium injection in the late phase of the discharge has reduced the central concentration of oxygen and other impurities, a result verified by unfolding ion densities from XUV charge exchange recombination measurements. Since it is clear that surface retention time for lithium is shorter than the duration of a single discharge, still better conditioning results can be expected fron the injection of pellets into the early phase of NCS discharges. The highest $Q_{d\text{-}d}$ and $n\tau T_i$ were obtained in DIII–D after Li pellet injection.

REFERENCES

[1]Tugarinov et.al., Rev. Sci. Instrum **66**, 603 (1995)

[2]Lerner, J.M. et.al., Flat Field Imaging Spectroscopy Using Aberration Corrected Holographic Gratings, in the Proc. of Symposium PIE, Vol. 278, p. 122, 1981.

[3]Lao, L.L. et.al., accepted for publication in May issue of Phys. Plasmas (1995); Rice, B.W. et al. accepted for publication in May issue of Phys. Plasmas(1995).

ACKNOWLEDGMENT

This is a report of work supported by the U.S. Department of Energy under Contract Nos. DE-AC03-89ER51114 and DE-AC05-96OR22464.